Available online at www.sciencedirect.com

SCIENCE DIRECT®

Journal of Nuclear Materials 352 (2006) 209–216

journal of nuclear materials

www.elsevier.com/locate/jnucmat

Improvement of the preparation of sintered pellets of thorium phosphate-diphosphate and associated solid solutions from crystallized precursors

N. Clavier [a], N. Dacheux [a,*], G. Wallez [b], M. Quarton [b]

[a] Groupe de Radiochimie, Institut de Physique Nucléaire, Bât. 100, Université Paris-Sud-11, 91406 Orsay, France
[b] Laboratoire de Cristallochimie du Solide, 4 place Jussieu, Université Pierre et Marie Curie, 75252 Paris, France

---

Abstract

Several compositions of thorium–uranium (IV) phosphate–hydrogenphosphate hydrate ($U_{x/2}Th_{2-x/2}(PO_4)_2$-$(HPO_4) \cdot H_2O$, TUPHPH) were prepared starting from actinides chloride solutions and concentrated phosphoric acid. The experimental synthesis parameters were optimized in order to get the quantitative precipitation of the cations and a good crystallization state. The extensive characterization of the solids demonstrated the existence of a complete solid solution between Th and U end-members and evidenced the good homogeneity of the powders. Their behaviors during heating treatment were then checked and confirm the formation of anhydrous thorium–uranium (IV) phosphate–hydrogenphosphate (TUPHP) and α-$U_xTh_{4-x}(PO_4)_4(P_2O_7)$ (α-TUPD) acting as intermediates. Finally, the low-temperature crystallized precursors were used in original sintering processes in order to improve the efficiency of the former cold-pressing sintering procedure.

PACS: 81.20.Ev; 28.41.Kw; 81.05

---

1. Introduction

The immobilization of radionuclides in an underground repository is actually considered as the most likely option in order to manage the long life and high activity radwaste. In this field, phosphate materials can be usually considered as potential host matrices for actinides. Indeed, several natural phosphate ores such as brabantites ($Ca_{0.5}M^{IV}_{0.5}PO_4$) [1,2], monazites ($M^{III}PO_4$) [3–5] or britholites (Ca_9Nd_{1-x}-$M^{IV}_x(PO_4)_{5-y}(SiO_4)_{1+y}F_2$) [6,7] can incorporate large amounts of uranium and/or thorium (up to 30 wt% in ThO_2) [3] and generally appear well-crystallized and resistant to aqueous alteration. In the last decade, several studies were also dedicated to the thorium phosphate-diphosphate (β-$Th_4(PO_4)_4P_2O_7$, β-TPD) [8–13] which appears as a promising material for the specific immobilization of tetravalent actinides since it allows the incorporation of uranium (up to 47.6 wt%), neptunium (33.2 wt%) and plutonium (26.1 wt%) by substitution of thorium in the crystal structure [11,12]. Moreover, the resulting

---

[*] Corresponding author. Tel.: +33 1 69 15 73 46; fax: +33 1 69 15 71 50.
E-mail address: dacheux@ipno.in2p3.fr (N. Dacheux).

0022-3115/$ - see front matter © 2006 Elsevier B.V. All rights reserved.
doi:10.1016/j.jnucmat.2006.02.056

solid solutions with actinides (β-$An_xTh_{4-x}(PO_4)_4(P_2O_7)$, β-TAnPD) exhibit good sintering properties [10,14] and present a strong resistance to aqueous corrosion [13].

Several chemical methods were already developed to perform the preparation of β-TPD and associated solid solutions including either wet and dry chemical processes [9]. The process based on the evaporation of a mixture of cations in acidic solutions and concentrated phosphoric acid led to single phase but heterogeneous solids after heating at high temperature [14]. Consequently, the synthesis of crystallized precursors of β-TPD and β-TUPD solid solutions i.e. thorium phosphate–hydrogenphosphate hydrate (TPHPH) [15] and associated $U_{x/2}Th_{2-x/2}(PO_4)_2(HPO_4) \cdot H_2O$ solid solutions (TUPHPH) [16], respectively, was performed in order to get dense and homogeneous solids at high temperature. We report in this paper some new features concerning the preparation, the characterization, and the sintering of these low-temperature crystallized precursors. First, the experimental conditions leading to the quantitative precipitation of the cations and to a good crystallization state were investigated during the synthesis. The XRD characterization of the samples was then performed on the basis of the last results obtained concerning the crystal structure in order to make the evidence of the existence of a complete solid solution between thorium and uranium end-members. After verification of the transformation scheme of the precursors during the heating treatment, their precipitation was applied to two original sintering processes with the aim to improve the initial cold-pressing procedure previously described [14].

2. Experimental

Concentrated thorium chloride solutions ($C \approx 1.8$ M) were issued from Rhône-Poulenc (France). Uranium chloride solution was obtained by dissolving uranium metal chips in 4 M hydrochloric acid. The initial solutions were diluted to reach a final concentration of 0.7 M for thorium and 1.1 M for uranium (IV). Other chemical reagents used for the syntheses and for analyses were of pro-analysis grade and supplied by Aldrich or Fluka.

High-temperature treatments were performed up to 1573 K in alumina boats in PYROX MDB 15 or HM 40 furnace with heating rates of 2–5 K min^{-1}, under inert atmosphere (argon) in order to avoid the oxidation of uranium (IV) into uranium (VI).

The XRD diagrams were collected with a Philips X'PERT-PRO-PW3040/60 or BRUKER D8 ADVANCE diffractometer system using Cu-K_α rays ($\lambda = 1.5418$ Å). The precise peaks positions were determined using the fitting program EVA, available in the software package Diffrac-AT V 3.0 purchased by Socabim and supplied by Siemens. μ-Raman absorption spectra were collected from room temperature to 573 K by means of a Dilor–Jobin Yvon apparatus using argon laser working at 514.5 nm. TGA and DTA experiments were done using a Setaram TG 92-16 apparatus, in alumina crucibles, under inert atmosphere (argon) with heating rates of 2–5 K min^{-1} and cooling rate of 20 K min^{-1}.

Electron probe microanalyses (EPMA) were carried out using a Cameca SX 50 apparatus with an acceleration voltage of 15 kV and a current of 10 nA considering the following calibration standards: $SmPO_4$ (K_α ray of phosphorus), ThO_2 (M_α ray of thorium) and $UO_{2.12}$ (M_β ray of uranium).

The densities of the sintered samples were evaluated using water ($\rho = 0.997$ g cm^{-3} at 298 K) after immersion and outgassing of the sample in the fluid or helium pycnometry. For measurements with helium, multi pycnometer from Quantachrome was used.

3. Results and discussion

3.1. Preparation of the samples

The precipitation of the precursors followed two methods involving an initial mixture of concentrated solutions of the cations considered and phosphoric acid in PTFE containers. The reagents were introduced in the stoichiometric conditions of the final ceramic expected, considering an excess of 2% in mole of H_3PO_4. For the first kind of syntheses, the closed container was put on a sand bath ($T = 423$ K) for several hours to four weeks. For hydrothermal syntheses, PTFE containers were placed in autoclaves supplied by Parr Instrument Company. This system was set in an oven at 433 K for about one month. Whatever the method considered, the solids obtained were separated from the supernatant by centrifugation at 3500 rpm, washed several times with deionized water then with ethanol in order to eliminate the remaining acid and finally dried. In order to obtain the quantitative precipitation of the tetravalent cations and a good crystallization state, the influence of the holding time and heating temperature on the synthesis of the

Table 1
Influence of the holding time and heating temperature on the precipitation of TPHPH[a]

Time (min)	15	30	60	75	90	150	210	450
393 K	+	+	+	+	+	+	+	p
403 K	+	+	+++	++++	++++	p	p	p
413 K	+	++	+++	++++	++++	p	p	p
423 K	+	++	++++	p	p	p	p	p
433 K	+	++	p	p	p	p	p	p
443 K	+	++	p	p	p	p	p	p

+: transparent gel.
++: beginning of the precipitation inside the gel, formation of opaque zones.
+++: slight precipitation, appearance of small crystals.
++++: significant conversion of gelatinous phase into white precipitate.
p: white precipitate.
[a] No modification compared to the initial mixture before 15 min of heating.

precursors was examined during the preparation of TPHPH on a sand bath (Table 1). For all the experimental conditions investigated, the formation of TPHPH occurred in four steps. First, heating the initial mixture of acidic solutions led to the formation of a gelatinous phase. Due to the high number of parameters driving the gelation, it was not possible to identify precisely the resulting phase. Nevertheless, in the media considered, several hydrolyzed phosphoric complexes like $[Th(OH)(H_2PO_4) \cdot 5H_2O]^{2+}$ or $[Th(OH)_2(H_2PO_4) \cdot 4H_2O]^{+}$ [17] could structurate this gelatinous phase. The apparition of opaque zones in the gel marked the beginning of the crystallization of TPHPH, which became much more visible after about 1 h of heating (formation of small white crystals). This precipitation induced the partial dehydration of the gel, thus its transformation into phosphoric acid [18]. The destructuration of the gelatinous phase finally led to a liquid phase containing the TPHPH white precipitate. The more important was the temperature, the shorter was the holding time required for the preparation of pure TPHPH: for example, a crystallized compound was obtained after only 1 h at 433 K. The influence of the temperature on the crystallization state of TPHPH was then investigated for various heating times through the variation of the full-width half-maximum (FWHM) of the main diffraction lines of the XRD pattern (Fig. 1). The highest crystallinity was reached after 3.5–7 h at 433 K. For longer times of precipitation (several days to few weeks), the crystallinity was slightly deteriorated while SEM observations exhibited a significant decrease of the crystal size associated to an increase of the specific surface area from about 3 $m^2 g^{-1}$ to 10–15 $m^2 g^{-1}$. On the basis of these results, the optimal conditions of preparation of TPHPH were fixed to $T = 433$ K and $t = 3.5$ h. Further studies are actually under progress in order to determine the optimal conditions of synthesis for the associated TUPHPH solid solutions: the first results do not reveal any change in the heating temperature but seem to indicate that a longer holding time is required.

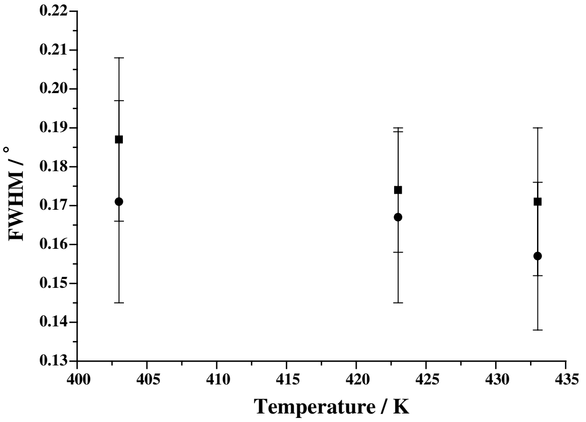

Fig. 1. Variation of the average FWHM versus temperature for $t = 3.5$ h (■) and $t = 7$ h (●).

3.2. Characterization of the precursors

3.2.1. EPMA experiments

The chemical composition and the homogeneity of several TUPHPH solid solutions were examined by the means of EPMA experiments (Table 2) then compared to that obtained for the TPHPH [15] and UPHPH [19] end-members. For all the samples analyzed, the elementary atomic percents and mole ratios appear consistent with that determined on the basis of the expected formula. Only small

Table 2
Results of EPMA experiments for several TUPHPH solid solutions

	x	Th/at.%	U/at.%	P/at.%	O/at.%	(U + Th)/P
Calculated[a]	**0.0**	11.8	0	17.6	70.6	0.67
EPMA [15]	0.0	12.1 ± 0.5	–	18.1 ± 0.3	69.7 ± 0.1	0.67 ± 0.02
Calculated[a]	**0.2**	11.2	0.6	17.6	70.6	0.67
EPMA	0.28 ± 0.08	11.2 ± 0.3	0.8 ± 0.2	18.3 ± 0.2	69.7 ± 0.1	0.66 ± 0.02
Calculated[a]	**0.4**	10.6	1.2	17.6	70.6	0.67
EPMA	0.32 ± 0.08	11.2 ± 0.3	1.0 ± 0.2	18.1 ± 0.2	69.7 ± 0.1	0.68 ± 0.02
Calculated[a]	**2**	5.9	5.9	17.6	70.6	0.67
EPMA	1.96 ± 0.04	6.1 ± 0.2	6.0 ± 0.2	18.2 ± 0.1	69.7 ± 0.1	0.67 ± 0.01
Calculated[a]	**2.4**	4.7	7.1	17.6	70.6	0.67
EPMA	2.28 ± 0.24	5.3 ± 0.7	7.0 ± 0.8	18.0 ± 0.4	69.7 ± 0.1	0.68 ± 0.04
Calculated[a]	**3.2**	2.4	9.4	17.6	70.6	0.67
EPMA	3.32 ± 0.04	2.1 ± 0.2	10.2 ± 0.2	17.9 ± 0.2	69.7 ± 0.1	0.68 ± 0.02
Calculated[a]	**4**	0	11.8	17.6	70.6	0.67
EPMA [19]	4	–	12.6 ± 0.3	17.7 ± 0.2	69.6 ± 0.1	0.71 ± 0.03

[a] The hydrogen and oxygen atoms belonging to the water molecule were not considered in the calculated value since they could not be directly analyzed by the method considered.

variations were noted for the U/(U + Th) = $x/4$ mole ratio, due to the small oxidation of tetravalent uranium (up to 5% in mole) during the precipitation and/or to the presence of small amount of uranium (VI) in the starting solution. Nevertheless, the cation/PO_4 mole ratio always remains equal to 2/3, indicating that neither the slight initial lack in tetravalent uranium (uranium (VI) not being precipitated in these experimental conditions) nor the excess of phosphoric acid introduced during the preparation modify the stoichiometry of the final precipitate. In all the operating conditions, the powders were found to be single phase and of improved homogeneity compared to the precursors prepared via the chemical way of reference, called 'direct evaporation' [16].

3.2.2. XRD experiments

XRD diagrams were collected for various chemical compositions of TUPHPH. Whatever the substitution rate x considered, the pattern recorded was found to be in good agreement with that of TPHPH [15] and UPHPH [19]. The powders appeared well-crystallized and no additional diffraction line was observed, confirming that the samples were single phase. In order to follow the progressive replacement of thorium by uranium (IV) in the crystal structure, the unit cell parameters were refined using the U-Fit software [20]. In a first time, the monoclinic structure reported in the literature for TPHPH (space group: $P2_1$; $Z = 2$) [21] was used, leading to the previously published results [16]. However, the refinement of the unit cell parameters was sometimes found to be difficult, especially for high x values. Thus, complementary studies concerning the structure of TPHPH and related compounds were undertaken: the crystal structures of U and Th end-members were found to be very close, TPHPH crystallizing in the orthorhombic system (*Cmcm* space group) and UPHPH in a slightly distorted monoclinic system with $\beta = 91.67°$ (*Cc* space group) [22]. Consequently, the unit cell parameters of TUPHPH solid solutions were refined considering both structures and plotted versus the substitution coefficient x (Fig. 2) and their associated variations were gathered in Table 3. As expected from the structures of both end-members, the value of the β angle is slightly affected by the substitution of thorium by uranium (IV). For $x \leqslant 2.0$, the β angle remains equal to 90° which corresponds to the

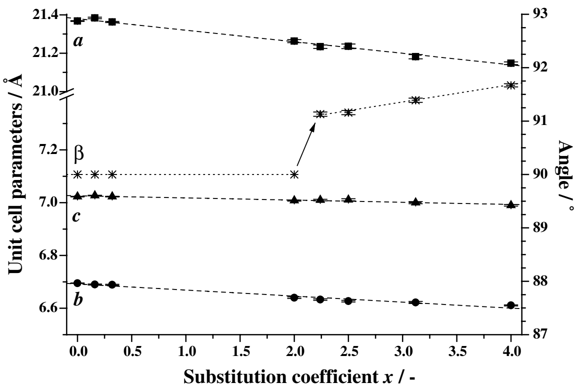

Fig. 2. Variation of the unit cell parameters a, b, c and of the β angle for $U_{x/2}Th_{2-x/2}(PO_4)_2(HPO_4) \cdot H_2O$ versus the x value.

Table 3
Variation of the unit cell parameters and associated volume of $U_{x/2}Th_{2-x/2}(PO_4)_2(HPO_4) \cdot H_2O$ versus the x value

a/Å		21.380(6) – 0.060(2) x_U
b/Å		6.692(4) – 0.023(2) x_U
c/Å		7.026(2) – 0.008(1) x_U
β/°	$x_U \leqslant 2.0$	90
	$x_U > 2.0$	90.39(6) + 0.32(2) x_U
V/Å^3		1005.3(6) – 7.5(3) x_U

orthorhombic structure. On the contrary, for $x > 2.0$, the β value increases versus the x value, leading to a monoclinic system. Nevertheless, the angle always remains close to 90° and the structure modification could be considered as a slight distortion of the initial orthorhombic lattice. All a, b and c parameters exhibit a small linear contraction when increasing the x value, which appears consistent with the variation of the ionic radius between thorium and uranium in the eight-fold coordination ($^{VIII}r_{Th} = 1.05$ Å, $^{VIII}r_U = 1.00$ Å) [23]. Moreover, this contraction appears to be limited since it reaches 1.0, 1.3 and 0.5% for a, b and c, respectively. In these conditions, the existence of a complete solid solution between TPHPH and UPHPH was confirmed.

3.3. Behavior of the precursors versus temperature

The chemical scheme of transformation from TUPHPH to β-TUPD solid solutions was previously evidenced through several physico-chemical techniques [16]. First, μ-Raman spectra were collected for various temperatures ranging from 298 to 1523 K (see Table 4). At room temperature, the spectra recorded appear in good agreement with that previously recorded for TPHPH [15]: all the vibration modes (δ_s, δ_{as}, ν_s, ν_{as}) of the P–O bond of the PO_4 group were observed in the 350–1200 cm^{-1} range [24] while the band pointed out around 910–935 cm^{-1} was correlated to the deformation of the P–O ⋯ H bond of the HPO_4 entity [25]. This last band disappears when heating above 523 K while additional bands located around 775 and 945 cm^{-1}, and correlated to the ν_s(P–O–P) and ν_{as}(P–O–P) vibration modes [26], respectively, arise progressively. These bands revealed the condensation of hydrogenphosphate groups into diphosphate entities when heating. Above 1223 K, the μ-Raman spectrum appears similar to that recorded for pure β-TPD [27].

From high-temperature XRD diagrams, different behaviors were observed above 873 K, depending on the substitution rate considered. For $x \leqslant 2.8$, the heating treatment led to homogeneous, single phase and well-crystallized β-TUPD solid solutions. In order to identify the successive reactions occurring during the heating treatment, TG and DT analyses were performed. As shown from Fig. 3, the total weight loss of 3.9%, observed between 323 K and 673 K, mainly occurred in two steps. Between 410 K and 490 K, the relative weight loss of 2.3% corresponded to the release of one water molecule per unit formula and was assigned to the full dehydration of TUPHPH, leading to the anhydrous TUPHP ($U_{x/2}Th_{2-x/2}(PO_4)_2(HPO_4)$). The loss of additional 1.0% ($0.5H_2O$) between 490 K and 570 K was correlated to the apparition of the ν_s(P–O–P) band in the μ-Raman spectra. This

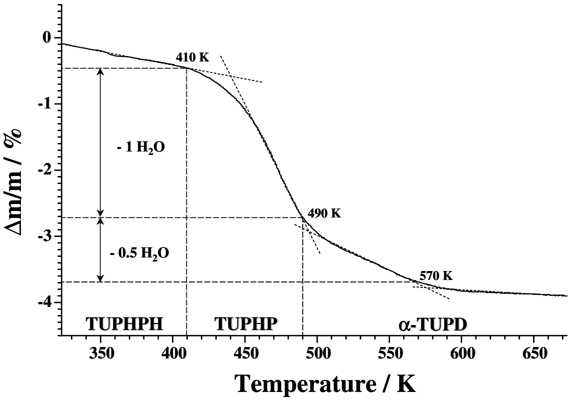

Fig. 3. TGA experiment recorded for $U_{0.8}Th_{1.2}(PO_4)_2(HPO_4) \cdot H_2O$.

Table 4
Assignment of the bands observed in the μ-Raman spectra (expressed in cm^{-1}) of TPHPH and TUPHPH ($x = 1.6$) versus the temperature

	δ_s (P–O)	δ_{as} (P–O)	ν_s (P–O–P)	ν_{as} (P–O–P)	ν_s (P–O)	δ_{op} (P–(O–H)) δ_{ip} (P–(O–H))	ν_{as} (P–O)
Room T	375–430	570–620	–	–	925	925	1020–1085
523 K	350–425	500–620	776	945	N.O.	–	1025–1145
1073 K	350–425	500–620	774	942	N.O.	–	1025–1155
1223 K	345–435	490–635	717, 734	920	N.O.	–	990–1280

N.O.: not observed.

accounted to the progressive condensation of hydrogenphosphate groups into diphosphate entities. In these conditions, the formation of a low-temperature form of TUPD, named α-TUPD ($U_xTh_{4-x}(PO_4)_4(P_2O_7)$), occurred between 490 K and 570 K. This form was found to be stable up to 1223 K where an exothermic peak on the DT curve shows its transformation into β-TUPD. This scheme of transformation appeared to be similar to that proposed from pure TPHPH [27].

On the contrary, polyphase systems were systematically obtained above 873 K for $x > 2.8$. The decomposition of the solid always led to a mixture of β-TUPD, $U_{2-y}Th_yO(PO_4)_2$ and α-$U_zTh_{1-z}P_2O_7$. On the basis of all these results, the chemical transformation of TPHPH and associated uranium-based solid solutions reported in Fig. 4 can be proposed.

3.4. Application to the preparation of β-TUPD sintered pellets

The preparation of β-TUPD solid solutions from the initial precipitation of TUPHPH was applied

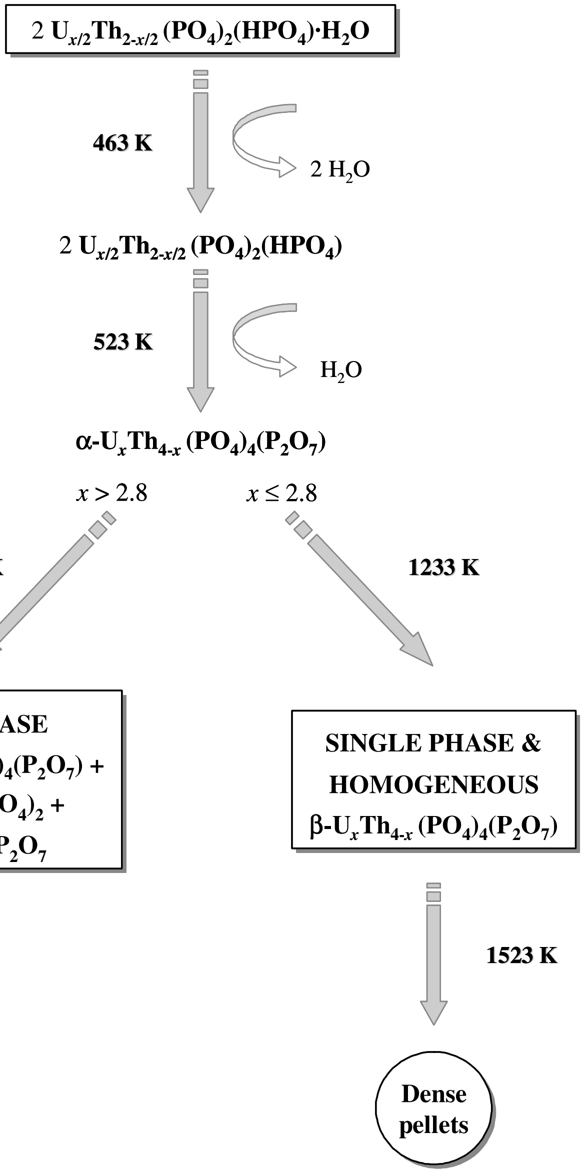

Fig. 4. Chemical scheme of transformation from TUPHPH to β-TUPD sintered pellets.

with success to the preparation of sintered pellets. Previous studies [14] showed that highly densified solids were obtained through a two-step procedure composed by an uniaxial pressing (100–800 MPa) at room temperature then a heating treatment at high temperature ($T = 1523$ K, $t = 10$ h, Ar). For all the samples, the density lain between 95% and 98% of the calculated value which corresponded to 2–5% of global porosity. EPMA experiments revealed an improved homogeneity in the repartition of the cations in the structure but a slight decomposition, consequently to the volatilization of P_4O_{10}, was noted at the surface of the pellet for high holding times (over than 20 h), leading to the formation of phosphate-depleted $U_{2-y}Th_yO(PO_4)_2$ phases. Consequently, complementary experiments were recently undertaken in order to improve the density of the pellets and to avoid any decomposition at the surface. Two processes were thus considered: for hot-pressing experiments, the powders were heated under inert atmosphere then pressed between 15 and 30 MPa at 1423 K. This lower operating temperature was sufficient to avoid any decomposition at the surface. The second kind of experiment started from a cold-pressed green pellet covered by powdered β-TPD or β-TUPD and heated at 1523 K under inert atmosphere. In this case, the presence of an inert powdered compound surrounding the green pellet acted as a protective layer and allowed to avoid the decomposition by shifting the equilibrium related to the volatilization of P_4O_{10}. The results obtained for both experiments (Table 5) were compared to that previously reported for classic cold-pressing procedure. As expected, the density of the pellets was significantly improved when using hot pressing, the global porosity being limited to 1–2%. Moreover, the specific surface area appeared very low and should delay the release of actinides during the leaching tests. The density was not modified in the second kind of experiments and no decomposition occurred at the surface of the pellet, even for high holding times (more than 20 h).

4. Conclusion

Several samples with general formula $U_{x/2}Th_{2-x/2}(PO_4)_2(HPO_4) \cdot H_2O$ ($0 \leqslant x \leqslant 4$) were synthesized as precursors of β-TUPD solid solutions by wet chemistry methods. The initial mixture of solutions led to the formation of a gelatinous phase which progressively turned into a crystallized precipitate. The experimental parameters were investigated and a heating treatment of only 5 h at 433 K allowed to reach the quantitative precipitation of the tetravalent cations in well-crystallized low-temperature precursors. Whatever the chemical composition considered, the powders were found to be homogeneous and single phase. Moreover, the existence of a complete solid solution between thorium and uranium (IV) end-members was evidenced through the XRD analysis. The solids present the orthorhombic structure of TPHPH for $x \leqslant 2.0$. Above this value, a slight distortion of the unit cell is observed and lead to a monoclinic structure.

The behavior of TUPHPH solid solutions during heating treatment was confirmed through several characterization techniques. The anhydrous TUPHP, as well as the low-temperature form of TUPD solid solutions, called α-TUPD, were evidenced as intermediate compounds. Complementary XRD experiments showed the decomposition of solids for $x > 2.8$ and allowed to propose a complete scheme of transformation of TUPHPH into β-TUPD sintered pellets. The preparation of such dense pellets from crystallized precursors was finally improved by the means of two original operating procedures. On the one hand, the use of a layer of inert powder surrounding the green pellet allowed to avoid the volatilization of P_4O_{10} at the surface of the sample, thus the formation of phosphate-depleted additional phases. On the other hand, hot-pressing method led to highly densified compounds, exhibiting a global porosity of only 1%.

All the results presented in this paper contributed to the significant improvement of the chemical

Table 5
Physico-chemical properties of β-TPD and β-TUPD pellets prepared through several sintering procedures

	T (K)	t (h)	$d/d_{Calc.}$ (%)[a]	Open porosity (%)	Close porosity (%)	Surface area (cm^2 g^{-1})	Vickers hardness (Hv)	Complementary observations
Cold pressing	1523	20	96	2	2	100–500	350–500	Partial surface decomposition
Hot pressing	1423	4	99	0	1	<100	N.D.	No decomposition
Cold pressing + powder	1523	20	96	2	2	100–500	350–500	No decomposition

[a] With an accuracy of 2%; N.D.: not determined.

procedure previously described. Consequently, the obtention of the quantitative precipitation of tetravalent cations during the synthesis, then the conversion of the low-temperature crystallized precursors into highly densified and homogeneous sintered pellets after heating treatment at high temperature, could be applied to the efficient decontamination of actinides-containing radioactive liquid waste. Several studies are now under progress in this aim and will be described soon.

References

[1] J.M. Montel, J.L. Devidal, D. Avignant, Chem. Geol. 191 (2002) 89.

[2] R. Podor, M. Cuney, C. Nguyen Trung, Am. Mineral. 80 (1995) 1261.

[3] L.A. Boatner, B.C. Sales, in: W. Lutze, R.C. Ewing (Eds.), Radioactive Waste Forms for the Future, North-Holland Physics, Amsterdam, 1998, p. 495.

[4] A. Meldrum, L.A. Boatner, W.J. Weber, R.C. Ewing, Geochim. Cosmochim. Acta 62 (1998) 2509.

[5] O. Terra, N. Clavier, N. Dacheux, R. Podor, New J. Chem. 27 (2003) 957.

[6] J. Carpena, F. Audubert, D. Bernache, L. Boyer, B. Donazzon, J.L. Lacout, N. Senamaud, in: I.G. McKinley, C. McCombie (Eds.), Scientific Basis for Nuclear Waste Management XXI, vol. 506, 1998, p. 543.

[7] R. Bros, J. Carpena, V. Sere, A. Beltritti, Radiochim. Acta 74 (1996) 277.

[8] P. Benard, V. Brandel, N. Dacheux, S. Jaulmes, S. Launay, C. Lindecker, M. Genet, D. Louër, M. Quarton, Chem. Mater. 8 (1996) 181.

[9] V. Brandel, N. Dacheux, M. Genet, Radiochemistry (Moscow) 43 (2001) 16.

[10] N. Dacheux, R. Podor, B. Chassigneux, V. Brandel, M. Genet, J. Alloys Compd. 271 (1998) 236.

[11] N. Dacheux, R. Podor, V. Brandel, M. Genet, J. Nucl. Mater. 252 (1998) 179.

[12] N. Dacheux, A.C. Thomas, V. Brandel, M. Genet, J. Nucl. Mater. 257 (1998) 108.

[13] A.C. Robisson, N. Dacheux, J. Aupiais, J. Nucl. Mater. 306 (2002) 134.

[14] N. Clavier, N. Dacheux, P. Martinez, E. du Fou de Kerdaniel, L. Aranda, R. Podor, Chem. Mater. 16 (2004) 3357.

[15] V. Brandel, N. Dacheux, M. Genet, R. Podor, J. Solid State Chem. 159 (2001) 139.

[16] N. Clavier, N. Dacheux, P. Martinez, V. Brandel, R. Podor, P. Le Coustumer, J. Nucl. Mater. 335 (2004) 397.

[17] V. Brandel, M. Genet, R. Guillaumont, New J. Chem. 13 (1989) 473.

[18] V. Brandel, G. Iroulart, E. Simoni, M. Genet, New J. Chem. 14 (1990) 113.

[19] V. Brandel, N. Clavier, N. Dacheux, J. Solid State Chem. 178 (2005) 1054.

[20] M. Evain, U-Fit Program, Institut des Matériaux de Nantes, France, 1992.

[21] M.A. Salvado, P. Pertierra, A.I. Bortun, C. Trobajo, J.R. Garcia, Inorg. Chem. 44 (2005) 3512.

[22] G. Wallez, M. Quarton, LCS–Université de Paris VI, France, private communication.

[23] R.D. Shannon, Acta Cryst. A 32 (1976) 751.

[24] P. Tarte, A. Rulmont, C. Merckaert-Ansay, Spectrochim. Acta A 42 (1986) 1009.

[25] M. Trchová, P. Čapková, P. Matějka, K. Melánová, L. Beneš, J. Solid State Chem. 145 (1999) 1.

[26] N. Khay, A. Ennaciri, J. Alloys Compd. 324 (2001) 800.

[27] N. Dacheux, N. Clavier, G. Wallez, V. Brandel, J. Emery, M. Quarton, M. Genet, Mater. Res. Bull. 40 (2005) 2225.